

Crystal and Electronic Structure of a Mixed-Valent Np(IV)–Np(V) Compound: [BuMelm]₅[Np(NpO₂)₃(H₂O)₆Cl₁₂]

Iraida Charushnikova,[†] Emilie Bossé,[‡] Dominique Guillaumont,[‡] and Philippe Moisy^{*‡}

[†]A. N. Frumkin Institute of Physical Chemistry and Electrochemistry, Russian Academy of Sciences, 31 Leninskiy pr., Moscow, 119991, Russia and [‡]CEA Marcoule, DEN/DRCP, BP 17171, 30207 Bagnols sur Cèze Cedex, France

Received July 31, 2009

A new mixed valent neptunium compound [BuMelm]₅[Np(NpO₂)₃(H₂O)₆Cl₁₂] was synthesized by evaporation of an ethyl acetate–acetone mixture where the salt [BuMelm]₂[NpCl₆] was dissolved. The crystal structure was determined using single crystal X-ray diffraction; it consists of four crystallographically unique Np centers with two different coordination environments in two different oxidation states. In addition, five crystallographically independent dialkylimidazolium cations stabilize the crystal through C–H···Cl hydrogen bonds. [Np(NpO₂)₃(H₂O)₆Cl₁₂] unit presents a highly symmetric structure with the formation of three Np(IV)–Np(V)O₂⁺ bonds. According to the crystal structure and density functional theory (DFT) calculations, the stability of the three Np⁴⁺–NpO₂⁺ interactions is due to the presence of chloride ions around NpO₂⁺ which brings electronic charge into the system and also to the presence of water molecules which create hydrogen bond with chloride ions.

Introduction

Room-temperature ionic liquids (RTILs) are remarkable solvents used in a large number of chemical processes including catalysis, organic synthesis, or electrochemistry.¹ They are composed of an organic cation (alkylimidazolium, alkylpyridinium, tetraalkylammonium, etc.) and an inorganic anion (Cl[−], AlCl₄[−], PF₆[−], (CF₃SO₂)₂N[−], etc.). Their physical and chemical properties can be modified by selecting the appropriate cation/anion combination.^{1d} Moreover, ionic liquids are relatively stable under radiation,² providing a unique opportunity to investigate actinide chemistry.

Long ignored, the presence of water becomes an important parameter in ionic liquids for their physicochemical properties and also for the chemical properties of actinides. As a function of the amount of water, it is possible to modify the direct environment of an actinide ion and to control its hydration sphere. For tetravalent actinides, to prevent variations in their environment and to avoid their hydrolysis, most

published studies in ionic liquids concern their hexachloride complexes.^{3,4} Furthermore, it has been shown that for hexachloride complexes, anionic complexes can be stabilized through hydrogen bonds involving chloride ions of the AnCl₆^{2−} anion and protons from the organic cation.^{5,6}

The solid-state chemistry of actinides is rich owing to the formation of numerous solids with Np(V) and U(VI) in which dioxocations NpO₂⁺ and UO₂²⁺ have the interesting property of participating in “cation–cation” interactions where oxygen atoms of dioxocations are also equatorial ligands of adjacent dioxocations.^{7,8} Cation–cation interaction was first discovered to occur in solution of U(VI) and Np(V)⁹ and later it was first observed in the crystal structure of sodium and Np(V) mellitate, Na₄[(NpO₂)₂C₆(COO)₆]·8H₂O.¹⁰ Interaction between NpO₂⁺ units is particularly well–documented in the solid state.^{7,10,11} In crystals it is an important structure-forming

*To whom correspondence should be addressed. E-mail: philippe.moisy@cea.fr.

(1) (a) Earle, M. J.; Seddon, K. R. *Pure Appl. Chem.* **2000**, *72*, 1391. (b) Hagiwara, R.; Lee, J. S. *Electrochemistry* **2007**, *75*, 23. (c) Welton, T. *Chem. Rev.* **1999**, *99*, 2071. (d) Wasserchied, P.; Welton, T. *Ionic liquids in synthesis*; Wiley-VCH: Weinheim, Germany, 2003.

(2) (a) Allen, D.; Baston, G.; Bradley, A. E.; Gorman, T.; Haile, A.; Hamblett, I.; Hatter, J. E.; Healey, M. J. F.; Hodgson, B.; Lewin, R.; Lovell, K. V.; Newton, B.; Pitner, W. R.; Rooney, D. W.; Sanders, D.; Seddon, K. R.; Sims, H. E.; Thied, R. C. *Green Chem.* **2002**, *4*, 152. (b) Berthon, L.; Nikitenko, S. I.; Bisel, I.; Berthon, C.; Faucon, M.; Saucerotte, B.; Zorz, N.; Moisy, P. *J. Chem. Soc., Dalton Trans.* **2006**, 2526. (c) Bossé, E.; Berthon, L.; Zorz, N.; Monget, J.; Berthon, C.; Bisel, I.; Legand, S.; Moisy, P. *Dalton Trans.* **2008**, 924.

(3) Cocalia, V. A.; Gutowski, K. E.; Rogers, R. D. *Coord. Chem. Rev.* **2006**, *250*, 755.

(4) Binnemans, K. *Chem. Rev.* **2007**, *107*, 2592.

(5) Nikitenko, S. I.; Hennig, C.; Grigoriev, M. S.; Le Naour, C.; Cannes, C.; Trubert, D.; Bossé, E.; Berthon, C.; Moisy, P. *Polyhedron* **2007**, *26*, 3136.

(6) Bossé, E.; Den Auwer, C.; Berthon, C.; Guilbaud, P.; Grigoriev, M. S.; Nikitenko, S.; Le Naour, C.; Cannes, C.; Moisy, P. *Inorg. Chem.* **2008**, *47*, 5746.

(7) Krot, N. N.; Grigoriev, M. S. *Russ. Chem. Rev.* **2004**, *73*, 89.

(8) Forbes, T. Z.; Wallace, C.; Burns, P. C. *Can. Mineral.* **2008**, *46*, 1623.

(9) Sullivan, J. C.; Zielen, A. J.; Hindman, J. C. *J. Am. Chem. Soc.* **1961**, *83*, 3373.

(10) Cousson, A.; Dabos, S.; Abazli, H.; Nectoux, F.; Pages, M.; Choppin, G. *J. Less-Common Met.* **1984**, *99*, 233.

(11) (a) Albrecht-Schmitt, T. E.; Almond, P. M.; Sykora, R. E. *Inorg. Chem.* **2003**, *42*, 3788. (b) Charushnikova, I. A.; Krot, N. N.; Polyakova, I. N. *Crystallogr. Rep.* **2006**, *51*, 201. (c) Forbes, T. Z.; Burns, P. C.; Soderholm, L.; Skanthakumar, S. *Chem. Mater.* **2006**, *18*, 1643. (d) Grigoriev, M. S.; Antipin, M. Y.; Krot, N. N. *Radiochemistry* **2006**, *48*, 6. (e) Almond, P. M.; Skanthakumar, S.; Soderholm, L.; Burns, P. C. *Chem. Mater.* **2007**, *19*, 280. (f) Grigoriev, M. S.; Krot, N. N.; Bessonov, A. A.; Suponitsky, K. Y. *Acta Crystallogr., Sect. E* **2007**, *63*, M561. (g) Charushnikova, I. A.; Krot, N. N.; Starikova, Z. A. *Radiochim. Acta* **2007**, *95*, 495. (h) Cornet, S. M.; Haller, L. J. L.; Sarsfield, M. J.; Collison, D.; Helliwell, M.; May, I.; Kaltsayannis, N. *Chem. Commun.* **2009**, 917.

factor and can lead to form the systems of cation–cation bonds in various combinations, where NpO_2^+ dioxocations can be involved in one or more (up to four) bonds.⁷

However, despite the variety of cation–cation bonds in the crystal structure of Np, interactions between Np(IV) and Np(V)O_2^+ have been only recently found in a selenite compound $\text{Np(NpO}_2)_2(\text{SeO}_3)_3$.¹² The structure consists of three different coordination environments for Np in a three-dimension channel structure with three crystallographically unique Np centers.

While investigating the structure of neptunium in the hydrophobic ionic liquid 1-butyl-3-methylimidazolium bis-(trifluoromethanesulfonyl)imide ($\text{BuMeImTf}_2\text{N}$), we have isolated a new mixed-valent Np(IV)/Np(V) compound. Herein, we report its characterization. Its structure has been determined from single crystal X-ray diffraction. Its electronic structure has been investigated through density functional theory (DFT) calculations to get further insight into the Np(IV)/Np(V) interaction.

Experimental Section

Synthesis. The new salt $[\text{BuMeIm}]_5[\text{Np(NpO}_2)_3(\text{H}_2\text{O})_6\text{Cl}_{12}]$ (**1**) was prepared from the solid $[\text{BuMeIm}]_2[\text{NpCl}_6]$ compound in the form of a fine dark orange-brown powder with a grain size ranging from about 10 to 100 μm that has already been described.¹³ This compound (100–200 mg) was dissolved (1 mL) in a 2/1 ethyl acetate/acetone mixture at atmospheric pressure with approximately 70% relative humidity. Under these conditions the water concentration was estimated between 0.01 and 0.1 M. After 5 to 6 days the solvent had completely evaporated, and we obtained with a low yield a small fraction of compound (**1**) and $[\text{BuMeIm}]\text{Cl}$ crystals. The solvent (ethyl acetate/acetone) was optimized to allow slow oxidation of Np(IV) to Np(V) by oxygen at very low water concentrations. Typically, for different proportions (or for another solvent such as acetonitrile and methanol) the evaporation rate was either too fast (1–2 days) or too slow (1–2 weeks), and compound (**1**) could not be isolated. It is important to note that handling crystals of (**1**) is extremely difficult because in contact with humidity they agglomerate, forming a viscous paste with a risk of contamination with ²³⁷Np. In view of these difficulties, it was not possible to measure the UV–visible and IR spectra in either transmission mode (diluted in solid NaCl or KBr pellets) or reflection mode. The crystal compatible with X-ray measurements was selected and mounted on a glass capillary with Paratone-N grease to prevent decomposition in the ambient air. X-ray analysis indicated a formula of $[\text{BuMeIm}]_5[\text{Np(NpO}_2)_3(\text{H}_2\text{O})_6\text{Cl}_{12}]$ (**1**).

X-ray Structural Analysis. X-ray diffraction analysis was carried out on a KappaCCD automated diffractometer (Enraf-Nonius (MoK α radiation, graphite monochromator).¹⁴ The unit cell parameters (Table 1) were determined from 10 images with $\Delta\varphi = 1^\circ$ and refined for the whole set of reflections¹⁵ obtained in the range $\theta = 1\text{--}27.5^\circ$. The crystal-to-detector distance was fixed at 27 mm. Empirical absorption corrections were applied to the experimental set of intensities from (**1**) (MULABS).¹⁶ The structure was solved by a heavy-atom method (SHELXS97) and refined by the full-matrix least-squares procedure (SHELXL97).¹⁷ The refinement in the anisotropic

Table 1. Crystallography

empirical formula	$\text{C}_{40}\text{H}_{87}\text{O}_{12}\text{N}_{10}\text{Cl}_{12}\text{Np}_4$
crystal system	triclinic
space group	$P\bar{1}$
<i>a</i> (Å)	14.5485(3)
<i>b</i> (Å)	14.8947(3)
<i>c</i> (Å)	20.7821(6)
α (deg)	86.8718(12)
β (deg)	70.2530(14)
γ (deg)	62.2690(12)
<i>V</i> (Å ³)	3723.14(15)
<i>Z</i>	2
ρ_c (g cm ^{−3})	2.028
R_1 [$I > 2\sigma(I)$]	0.0568, 0.1416
R_1, wR_2 (all data)	0.0945, 0.1572

approximation for all non-hydrogen atoms indicated that atoms of organic BuMeIm^+ cations have high temperature factors, especially for C atoms of CH_3 groups. Finally the positions of C atoms were refined with fixed U_{ij} parameters and fixed C–C bonds of methyl groups equal to 1.53(2) Å. The H atoms of BuMeIm^+ cations were determined geometrically and refined isotropically by the riding model with displacement parameters equal to 1.2 (CH , CH_2) and 1.5 (CH_3) times those of the attached carbon atoms. The coordinates of the H atoms of the water molecules were found on Fourier maps. Their positional and thermal parameters were refined with $U_{\text{H}} = 1.2U_{\text{eq}}(\text{O})$ and fixed bond lengths equal to 0.85(5) Å.

Computational Details. The geometries, harmonic frequencies, and bonding analysis have been calculated at the DFT level with the Gaussian 03 package.¹⁸ The calculations were performed using relativistic effective core potentials (RECP). Spin–orbit effects were neglected. A small-core energy-adjusted RECP developed in the Stuttgart and Dresden groups¹⁹ was used for neptunium atoms together with the accompanying segmented basis set to describe the valence electron density. The valence basis set is (14s13p10d8f), basis contracted to [10s9p5d4f] for neptunium. On other atoms, a 6-31G* basis set was used. The systems are open-shell, and DFT calculations were performed within the unrestricted Kohn–Sham formalism on high-spin configurations. The hybrid B3LYP was employed. In Gaussian 03, non-defaults ultrafine integration grids and tight energy convergence criteria were used. For the larger system, calculations were performed by using different starting guesses for the wave function corresponding to different 5f orbital occupations.

Previous calculations on actinyl systems (closed or open shell) have shown that structural parameters and vibrational frequencies can be correctly determined using DFT calculations²⁰ with B3LYP and a 6-31G* basis set.²¹ Spin–orbit effects and multiplet splitting are expected to be significant for high-spin open-shell actinide systems but not for structural parameters or vibrational frequencies.^{22,23}

Harmonic vibrational frequencies were calculated analytically to show that the optimized structures are true minima.

A Natural Bond Orbital (NBO) Analysis were performed using the NBO 5.0 software²⁴ from wave functions obtained with Gaussian 03 at the RECP/B3LYP level of calculation.

(18) Frisch, M. J. et al. *Gaussian 03*, Revision D.02; Gaussian, Inc.: Wallingford, CT, 2004.

(19) Cao, X. Y.; Dolg, M.; Stoll, H. *J. Chem. Phys.* **2003**, *118*, 487.

(20) Ismail, N.; Heully, J. L.; Saue, T.; Daudey, J. P.; Marsden, C. J. *Chem. Phys. Lett.* **1999**, *300*, 296.

(21) (a) Hay, P. J.; Martin, R. L.; Schreckenbach, G. *J. Phys. Chem., Sect. A* **2000**, *104*, 6259. (b) Hay, P. J.; Martin, R. L. *J. Chem. Phys., Sect. A* **1998**, *109*, 3875. (c) Guillaumeont, D. *J. Phys. Chem., Sect. A* **2004**, *108*, 6893.

(22) Kerridge, A.; Kaltsoyannis, N. *J. Phys. Chem., Sect. A* **2009**, *113*, 8737.

(23) Clavaguera-Sarrio, C.; Vallet, V.; Maynau, D.; Marsden, C. J. *J. Chem. Phys.* **2004**, *121*, 5312.

(24) Glendening, E. D. B. J. K.; Reed, A. E.; Carpenter, J. E.; Bohmann, J. A.; Morales, C. M.; Weinhold, F. *NBO 5.0*; Theoretical Chemistry Institute, University of Wisconsin: Madison, WI, 2001.

(12) Almond, P. M.; Sykora, R. E.; Skanthakumar, S.; Soderholm, L.; Albrecht-Schmitt, T. E. *Inorg. Chem.* **2004**, *43*, 958.

(13) Nikitenko, S. I.; Moisy, P. *Inorg. Chem.* **2006**, *45*, 1235.

(14) *Nonius KappaCCD Software*; Bruker Nonius BV: Delft, The Netherlands, 1998.

(15) Otwinowski, Z.; Minor, W. *Macromolecular Crystallography*; Academic Press: New York, 1997; Vol. 276.

(16) Blessing, R. H. *Acta Crystallogr., Sect. A* **1995**, *51*, 33.

(17) Sheldrick, G. M. *Acta Crystallogr., Sect. A* **2008**, *64*, 112.

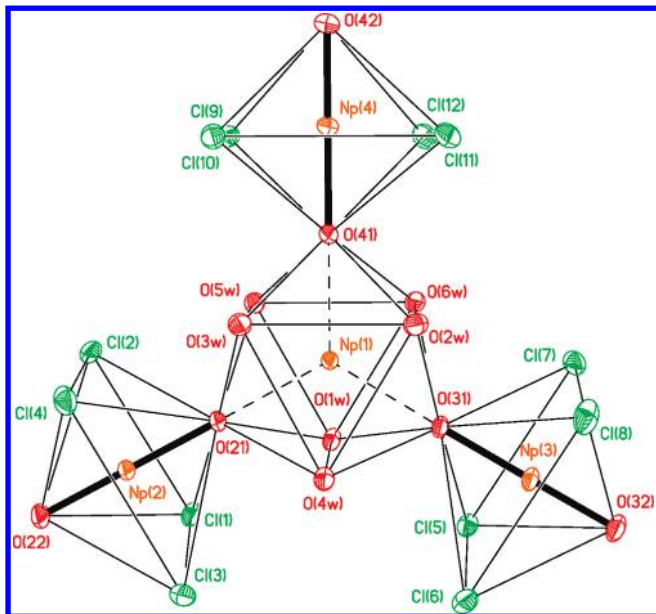


Figure 1. View of $[\text{Np}(\text{NpO}_2)_3(\text{H}_2\text{O})_6\text{Cl}_{12}]^{5-}$ in **(1)**. Dashed lines represent cation–cation bonds.

NBO analysis may depend upon the partitioning of atomic orbitals between core, valence, and rydberg.²⁵ Following Clark et al.,²⁶ 5f, 6d, and 7s subshells of neptunium were considered as valence orbitals because the ground-state atomic configuration of neptunium contains 5f, 6d, and 7s electrons.

Results and Discussions

Figure 1 displays the X-ray crystal structure of $[\text{Np}(\text{NpO}_2)_3(\text{H}_2\text{O})_6\text{Cl}_{12}]^{5-}$ where one Np^{4+} interacts with three NpO_2^+ units. $[\text{Np}(\text{NpO}_2)_3(\text{H}_2\text{O})_6\text{Cl}_{12}]$ adopts a highly symmetrical structure with a symmetry point group close to D_{3h} . The three neptunyl dioxocations act as monodentate ligands toward Np^{4+} . As a result, the mixed-valent cation $[\text{Np}(\text{NpO}_2)_3]^{7+}$ is formed (see Supporting Information, Figure S1). The coordination number of tetravalent $\text{Np}(\text{I})$ atom is 9, and its coordination polyhedron is a tricapped trigonal prism (Figure 1). Six water molecules are placed at the vertices of a trigonal prism (the average $\text{Np}(\text{I})\text{—O}_w$ bond length is 2.456 Å). Tetragonal faces of prism are centered by three “yl” oxygen atoms of dioxocations NpO_2^+ (the average $\text{Np}(\text{I})\text{—O}_{\text{yl}}$ bond length is 2.288 Å). Intermolecular hydrogen bonds are formed between chloride ions and water hydrogen atoms ($\text{H}\cdots\text{Cl}$ distances range from 2.33 to 2.68 Å, Figure 2) which can stabilize the cation–cation complex. The coordination polyhedra of the three crystallographically unique neptunyl Np centers, $\text{Np}(\text{2})$, $\text{Np}(\text{3})$, and $\text{Np}(\text{4})$, are tetragonal bipyramidal (Figure 1) with oxygen atoms in apical positions. $\text{Np}(\text{IV})\cdots\text{Np}(\text{V})$ distances range from 4.160 to 4.183 Å with $\text{Np}(\text{IV})\text{—O—Np}(\text{V})$ angles very close to linearity.

The participation of dioxocations NpO_2^+ in cation–cation interaction as monodentate ligands results in noticeable difference in the two $\text{Np}=\text{O}$ bond distances of each NpO_2^+ unit (Table 2). The two bond lengths, averaged over the three dioxocations, are 1.887 and 1.790 Å, the difference between the two distance is 0.097 Å. This value is comparable to what

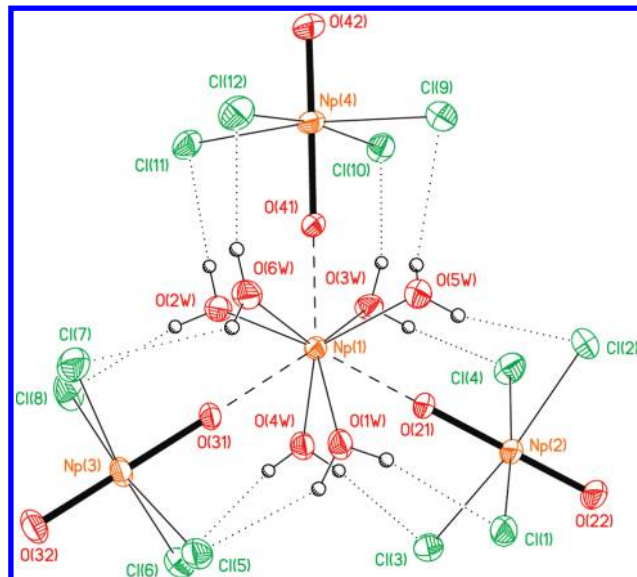


Figure 2. Intermolecular hydrogen bonds of $\text{O—H}\cdots\text{Cl}$ type in $[\text{Np}(\text{NpO}_2)_3(\text{H}_2\text{O})_6\text{Cl}_{12}]^{5-}$ complex anion (dotted lines).

was found in UO_2^+ tetramers where uranyl distances in each UO_2^+ unit differ by about 0.11 Å.²⁷ In previously reported $\text{Np}(\text{V})$ compounds with cation–cation interactions, the mean difference was 0.04 Å.⁷

The $\text{Np}(\text{2})$, $\text{Np}(\text{3})$, and $\text{Np}(\text{4})$ atoms are bound to four chloride anions in the equatorial plane with an average Np—Cl bond distance of 2.734 Å. A similar arrangement of Cl anions in the vertices of the square equatorial plane of $\text{Np}(\text{V})$ bipyramid has been found in the structure of $\text{Cs}_3\text{NpO}_2\text{Cl}_4$.²⁸ In $\text{Cs}_3\text{NpO}_2\text{Cl}_4$,^{28b} Np—Cl distances range from 2.758(3) to 2.759(3) Å, and $\text{Np}=\text{O}$ bond length is 1.828(5) Å. Despite of noticeable differences in $\text{Np}=\text{O}$ bond lengths of each NpO_2^+ cation in **(1)**, the mean value (1.838 Å) is comparable to that found in $\text{Cs}_3\text{NpO}_2\text{Cl}_4$.

In the previously reported $\text{Np}(\text{V})/\text{Np}(\text{IV})$ compound,¹² $\text{Np}(\text{NpO}_2)_2(\text{SeO}_3)_3$ formed a three-dimension channel structure with three crystallographically unique Np centers and three coordination environments in two different oxidation states. $\text{Np}(\text{IV})\cdots\text{Np}(\text{V})$ distances range from 4.00 to 4.18 Å and are comparable to those determined in **(1)**. In $\text{Np}(\text{NpO}_2)_2(\text{SeO}_3)_3$, $\text{Np}(\text{IV})$ is eight-coordinated and form a distorted NpO_8 dodecahedron with Np—O distances ranging from 2.31 to 2.40 Å. It is noteworthy that in **(1)** $\text{Np}^{4+}\text{—O}(\text{NpO}_2^+)$ distances are ~ 0.1 Å shorter even though $\text{Np}(\text{IV})$ is nine-coordinated. It is possible to explain this interesting fact by the presence of chloride ions in **(1)**. They can donate electronic charge to NpO_2^+ and to oxygen atoms. As a result, monodentate NpO_2^+ cations may become stronger ligands than those in $\text{Np}(\text{NpO}_2)_2(\text{SeO}_3)_3$. This point will be further discussed below with the results of the DFT calculations.

Five crystallographically independent dialkylimidazolium cations are found in **(1)**, which differ only in the conformation of the butyl-chain (Figure 3 and see Supporting Information, Figure S2). In previous X-ray structural investigation of $\text{An}(\text{IV},\text{VI})$ complexes crystallized from ionic liquids, the

(27) Burdet, F.; Pecaut, J.; Mazzanti, M. *J. Am. Chem. Soc.* **2006**, *128*, 16512.

(28) (a) Alcock, N. W.; Roberts, M. M.; Brown, D. *Acta Crystallogr., Sect. B* **1982**, *38*, 1805. (b) Lychev, A. A.; Mashirov, L. G.; Smolin, Y. I.; Shepelev, Y. F. *Radiokhimiya* **1988**, *30*, 388.

(25) Maseras, F.; Morokuma, K. *Chem. Phys. Lett.* **1992**, *195*, 500.

(26) Clark, A. E.; Sonnenberg, J. L.; Hay, P. J.; Martin, R. L. *J. Chem. Phys.* **2004**, *121*, 2563.

Table 2. Selected Interatomic Distances (Å) and Bond Angles (deg) for $[\text{Np}(\text{NpO}_2)_3(\text{H}_2\text{O})_6\text{Cl}_{12}]^{5-}$ from X-ray Structure (1) and DFT Calculations

distance	X-ray	calc.
Np(1)–O(21)	2.299(6)	2.332
Np(1)–O(31)	2.307(6)	2.337
Np(1)–O(41)	2.258(6)	2.429
Np(1)–O(1w)	2.451(7)	2.498
Np(1)–O(2w)	2.439(7)	2.470
Np(1)–O(3w)	2.433(8)	2.470
Np(1)–O(4w)	2.469(8)	2.498
Np(1)–O(5w)	2.481(8)	2.470
Np(1)–O(6w)	2.465(8)	2.470
Np(2)–O(21)	1.884(6)	1.922
Np(2)–O(22)	1.799(7)	1.805
Np(2)–Cl(1)	2.751(3)	2.814
Np(2)–Cl(2)	2.718(3)	2.809
Np(2)–Cl(3)	2.766(3)	2.814
Np(2)–Cl(4)	2.720(3)	2.809
Np(3)–O(31)	1.874(6)	1.921
Np(3)–O(32)	1.788(7)	1.805
Np(3)–Cl(5)	2.734(3)	2.815
Np(3)–Cl(6)	2.752(4)	2.815
Np(3)–Cl(7)	2.713(4)	2.810
Np(3)–Cl(8)	2.713(3)	2.810
Np(4)–O(41)	1.902(6)	1.896
Np(4)–O(42)	1.784(8)	1.807
Np(4)–Cl(9)	2.728(3)	2.830
Np(4)–Cl(10)	2.747(3)	2.830
Np(4)–Cl(11)	2.740(3)	2.830
Np(4)–Cl(12)	2.727(4)	2.830
angle	X-ray	calc.
O(21)Np(1)O(31)	120.2(2)	120.1
O(21)Np(1)O(41)	118.3(2)	119.9
O(31)Np(1)O(41)	121.6(2)	119.8
O(21)Np(2)O(22)	179.2(4)	179.6
Np(1)O(21)Np(2)	179.7(4)	179.9
O(31)Np(3)O(32)	178.1(4)	179.6
Np(1)O(31)Np(3)	179.1(4)	179.6
O(41)Np(4)O(42)	178.8(4)	179.6
Np(1)O(41)Np(4)	179.9(4)	179.7

crystal structures of $[\text{BuMeIm}]_2[\text{UCl}_6]$ and $[\text{MeBu}_3\text{N}]_2[\text{UCl}_6]$,⁶ $[\text{EtMeIm}]_2[\text{UCl}_6]$ and $[\text{EtMeIm}]_2[\text{UO}_2\text{Cl}_4]$ ²⁹ or $[\text{BuMeIm}]_2[\text{UO}_2\text{Cl}_4]$ ⁷ were obtained where MeBu_3N is methyltributylammonium and EtMeIm is 1-ethyl-3-methylimidazolium. The existence in the crystals of $\text{C}-\text{H}\cdots\text{Cl}$ hydrogen bonds and their influence on crystal packing were largely discussed. In crystal (1), there are seven short hydrogen-bond contacts between 1,3-dialkylimidazolium cations and adjacent Cl anions (see Supporting Information, Figure S2). Three of them with acidic ring-hydrogens of C(1), C(25), and C(33) atoms are equal to 2.84, 2.75, and 2.70 Å, respectively. The remaining four contacts are with H atoms from CH_3 and C_4H_9 groups (with distances equal to 2.61 Å for atom C(28), 2.76 Å for atom C(37), 2.82 Å for atom C(28), and 2.84 Å for atom C(30)). In addition, there are 10 contacts in the range 2.88–2.94 Å, which are below the van der Waals contact limit (2.95 Å³⁰). Such interactions can be classified as extremely weak H-bonds. The flexibility of the butyl-chain within BuMeIm cations allows a close packing of the fragment

structure. Therefore, it provides short contacts between not only acidic hydrogen atoms, but also between the low acidity hydrogen donors. In other words, the conformational flexibility of 1,3-dialkylimidazolium cations arising from their butyl-chains help to stabilize the crystal lattice via a combination of coulombic ion–ion interaction, $\text{C}-\text{H}\cdots\text{Cl}$ hydrogen bonds, and van der Waals forces.

To get further insight into $\text{Np}^{4+}-\text{NpO}_2^+$ interaction, the geometries and electronic structures were calculated for the solid state structure without dialkylimidazolium cations and for model structures. Starting from the X-ray structure of $[\text{Np}(\text{NpO}_2)_3(\text{H}_2\text{O})_6\text{Cl}_{12}]^{5-}$, a geometry optimization was performed, and it resulted in a stable structure (no imaginary frequencies) with $\text{Np}(\text{IV})-\text{Np}(\text{V})$ distances ranging from 4.26 to 4.32 Å. Calculated and crystal geometrical parameters are compared in Table 2. All calculated bond distances are longer than in the crystal structure (up to 0.1 Å). This can be attributed to the large negative charge of the system which is not screened by the crystal environment in the calculation. In particular, we should have a better agreement between calculated and crystal bond lengths by including dialkylimidazolium cations in the calculation. But it is very difficult to achieve the energy convergence of such open-shell high-spin systems with four neptunium atoms, and it was not possible to include screening effects in the calculations. However, despite the limitations of the calculation, we were able to obtain a stable structure with $\text{Np}^{4+}-\text{O}(\text{NpO}_2^+)$ bonds in the range of what is seen in the crystal (2.3–2.4 Å). Besides, as observed in the X-ray structure, the calculation gave two different $\text{Np}(\text{V})-\text{O}$ bond lengths in each NpO_2^+ unit, which differ by 0.1 Å. Calculated $\text{Np}(\text{IV})-\text{Ow}$ distances are very closed to the experimental values whereas $\text{Np}(\text{V})-\text{Cl}$ distances are slightly overestimated by the calculations. In the calculated structure, the six water molecules form twelve hydrogen bonds with the chloride as deduced from the X-ray structure. An unexpected result is that in the calculation we obtained two short and one long $\text{Np}(\text{IV})-\text{O}$ distances whereas in the crystal structure one short and two long distances are found. $\text{Np}(\text{IV})$ ion is a $5f^3$ open-shell ion, and the system has several low-lying electronic states because of the near-degeneracy of the $5f$ shell. The $\text{Np}(\text{IV})-\text{O}$ distance could be influenced by the symmetry of the singly occupied $5f$ orbitals. We did geometry optimizations for different electronic configuration of $\text{Np}(\text{IV})$ corresponding to various symmetries of the singly occupied $5f$ orbitals. We were able to obtain a higher energy structure which had three equal $\text{Np}(\text{IV})-\text{O}$ distances of 2.35 Å. Thus, $\text{Np}-\text{O}$ distances are related to the electronic ground state configuration of the $5f$ shell of $\text{Np}(\text{IV})$. Still, only higher level multiconfigurational calculations, possibly with spin–orbit effects, could help to overcome the defect of the DFT calculations to determine unambiguously the electronic ground state configuration of $\text{Np}(\text{IV})$ in the system and its relation with $\text{Np}(\text{IV})-\text{O}$ distances. Unfortunately, these types of calculations are currently unfeasible on such a large system.

To further understand the role of chloride ions and chloride-water hydrogen bonds for the stability of $\text{Np}^{4+}-\text{NpO}_2^+$ interactions, we performed additional geometry optimizations starting from the optimized structure of $[\text{Np}(\text{NpO}_2)_3(\text{H}_2\text{O})_6\text{Cl}_{12}]^{5-}$ and removing chloride ions, water molecules, or both. We started by keeping only the mixed-valent cation $[\text{Np}(\text{NpO}_2)_3]^{7+}$, but the $\text{Np}(\text{IV})-\text{O}$ bond distance elongates up to dissociation. Keeping the six

(29) (a) Hitchcock, P. B.; Mohammed, T. J.; Seddon, K. R.; Zora, J. A.; Hussey, C. L.; Ward, E. H. *Inorg. Chim. Acta* **1986**, *113*, L25. (b) Deetlefs, M.; Hussey, C. L.; Mohammed, T. J.; Seddon, K. R.; van Den Berg, J. A.; Zora, J. A. *J. Chem. Soc., Dalton Trans.* **2006**, 2334.

(30) Bondi, A. J. *Phys. Chem.* **1964**, *68*, 441.

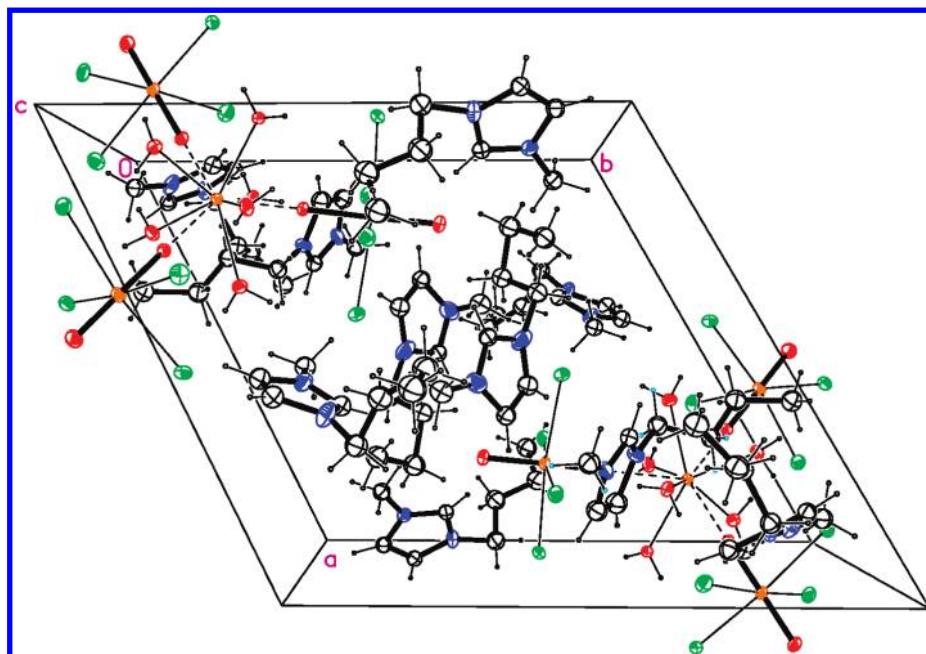


Figure 3. Packing diagram of the structure (1) (dashed lines show cation–cation bonds).

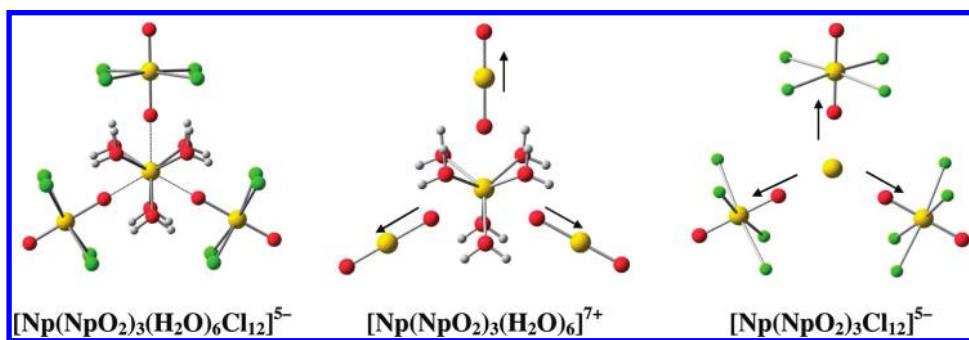


Figure 4. Geometry optimizations of $[\text{Np}(\text{NpO}_2)_3(\text{H}_2\text{O})_6\text{Cl}_{12}]^{5-}$, $[\text{Np}(\text{NpO}_2)_3(\text{H}_2\text{O})_6]^{7+}$, and $[\text{Np}(\text{NpO}_2)_3\text{Cl}_{12}]^{5-}$. The arrows indicate the elongation of Np(IV)–O bond up to dissociation upon geometry optimization.

water molecules without the chloride ions or the water molecules without the chlorides also leads to the dissociation of the complex. $[\text{Np}(\text{NpO}_2)_3(\text{H}_2\text{O})_6]^{7+}$ dissociates into $[\text{Np}(\text{H}_2\text{O})_6]^{4+}$ and NpO_2^+ subspecies and $[\text{Np}(\text{NpO}_2)_3\text{Cl}_{12}]^{5-}$ dissociates into Np^{4+} and $[\text{NpO}_2\text{Cl}_4]^{3-}$. This confirms the key role of both chloride ions and water molecules for the stability of the complex (Figure 4).

Vibrational frequencies were calculated for $[\text{Np}(\text{NpO}_2)_3(\text{H}_2\text{O})_6\text{Cl}_{12}]^{5-}$ and $[\text{NpO}_2\text{Cl}_4]^{3-}$. For $[\text{NpO}_2\text{Cl}_4]^{3-}$, $\text{O}=\text{Np}=\text{O}$ stretching frequencies are calculated as 791 cm^{-1} (symmetric mode) and 861 cm^{-1} (antisymmetric mode). For $[\text{Np}(\text{NpO}_2)_3(\text{H}_2\text{O})_6\text{Cl}_{12}]^{5-}$, because of the two different Np(V)–O distances, the antisymmetric stretching mode is mainly localized on the shorter Np(V)–O bond whereas the lower energy symmetric mode is localized on the longest Np(V)–O bond. In addition the symmetric mode is coupled with some libration modes of the water molecules, which results in the splitting of this mode in a wide range, from 654 to 741 cm^{-1} . The antisymmetric mode is calculated at 828 , 829 , and 836 cm^{-1} . The comparison of calculated stretching frequencies in $[\text{Np}(\text{NpO}_2)_3(\text{H}_2\text{O})_6\text{Cl}_{12}]^{5-}$ and $[\text{NpO}_2\text{Cl}_4]^{3-}$ clearly shows the weakening of the Np(V)–O bond upon binding to Np(IV).

Table 3 shows electronic charges for selected atoms and for NpO_2 and H_2O subspecies as inferred from the NBO population analysis. The results for the complex are compared to those calculated in the isolated NpO_2^+ and $[\text{NpO}_2\text{Cl}_4]^{3-}$ species. The NBO analysis assigns an atomic charge of 1.85 to Np(IV) which is much less than its formal charge of 4. This shows a strong charge transfer of about 2.2 e^- from the other subspecies toward the central Np(IV) atom. According to NBO analysis, 1.4 e^- originates from the three $[\text{NpO}_2\text{Cl}_4]^{3-}$ and 0.8 e^- from the six water molecules. The chlorine atomic charge is significantly less negative in (1) than in isolated $[\text{NpO}_2\text{Cl}_4]^{3-}$ by 0.2 e^- for each atom. This results in a smaller charge on Np(V) (1.3 instead of 1.8 in isolated $[\text{NpO}_2\text{Cl}_4]^{3-}$) and in a slightly negatively charged neptunyl species in the complex (-0.1 e^-) which favors its interaction with Np(IV) by diminishing the electrostatic repulsion. According to NBO atomic populations, the charge transfer toward Np(IV) is directed toward $6d$, $5f$, and $7s$ vacant orbitals as given by its population analysis (Table 3).

NBO calculates three donor–acceptor bonds between Np(IV) and the three oxygen atom from each NpO_2^+ . They correspond to σ -bonds which are highly polarized toward oxygen atoms (with less than 10% atomic orbital

Table 3. Calculated Electronic Charges for Selected Atoms (Np, O, and Cl) and Fragments (NpO_2 and H_2O) in Isolated NpO_2^+ , $[\text{NpO}_2\text{Cl}_4]^{3-}$ and in $[\text{Np}(\text{NpO}_2)_3(\text{H}_2\text{O})_6\text{Cl}_{12}]^{5-}$ (Natural Population Analysis)^a

	NpO_2^+	$[\text{NpO}_2\text{Cl}_4]^{3-}$	$[\text{Np}(\text{NpO}_2)_3(\text{H}_2\text{O})_6\text{Cl}_{12}]^{5-}$
Np^{IV}			+1.85 (5f ^{3.7} 6d ^{1.0} 7s ^{0.2})
Np^{V}	+2.18 (5f ^{4.1} 6d ^{0.9} 7s ^{0.0})	+1.64 (5f ^{4.0} 6d ^{1.2} 7s ^{0.2})	+1.33 (5f ^{4.0} 6d ^{1.4} 7s ^{0.3})
$\text{Np}^{\text{V}}\text{O}_2$	+1.00	+0.16	-0.10
O_{yl}	-0.59	-0.74	-0.65
$\text{O}_{\text{yl}}(\text{Np}^{\text{IV}})$			-0.78
Cl		-0.79	-0.61
H_2O			+0.13

^a Natural atomic populations are also reported for neptunium atoms in parentheses.

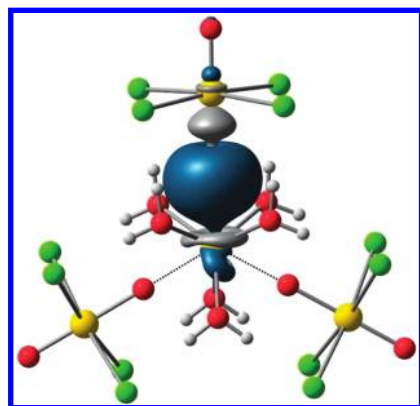


Figure 5. Schematic representation of the natural localized molecular orbital corresponding to one of the three σ $\text{Np}(\text{IV})\text{--O}$ bonds in $[\text{Np}(\text{NpO}_2)_3(\text{H}_2\text{O})_6\text{Cl}_{12}]^{5-}$. Neptunium(IV) natural atomic orbital contribution is 10% (7s(9%), 6d(55%), 5f(36%)), oxygen contribution is 90% (2s(62%), 2p(38%)).

contribution for neptunium, Figure 5) and which might alternatively be described as charge-transfer interactions. Only vacant 7s, 6d, and 5f orbitals of $\text{Np}(\text{IV})$ contribute in $\text{Np}(\text{IV})\text{--O}$ σ bonding. The weakening of one $\text{Np}(\text{V})\text{=O}$ bond upon binding to $\text{Np}(\text{IV})$ can also be seen in the bonding analysis. For NpO_2^+ fragment, NBO analysis attributes two $\text{Np}\text{--O}$ triple bonds polarized toward the oxygen. In $[\text{NpO}_2\text{Cl}_4]^{3-}$, the two $\text{Np}(\text{V})\text{=O}$ bonds are equivalent, and the Np atomic contribution is 20% for π bonds and 23% for σ -bonds. In $[\text{Np}(\text{NpO}_2)_3(\text{H}_2\text{O})_6\text{Cl}_{12}]^{5-}$, the orbital composi-

tion of the $\text{Np}^{4+}\text{--O}(\text{NpO}_2^+)$ bonds involving a non-coordinating O atom is unchanged (within 1%) compared to free $[\text{NpO}_2\text{Cl}_4]^{3-}$ whereas the Np contributions to the other $\text{Np}(\text{V})\text{--O}$ bonds decrease from 20 to 15% for π bonds and from 23% to 16% for σ -bonds.

Conclusion

In conclusion, we have characterized a new mixed-valent $\text{Np}(\text{IV})/\text{Np}(\text{V})$ complex cation which has been derived from the $\text{BuMeImTf}_2\text{N}$ ionic liquid and where three NpO_2^+ cations act as monodentate ligands toward one Np^{4+} center. According to the single crystal structure, the anionic neptunium cluster adopts a highly symmetric structure (pseudo D_{3h}). Each NpO_2^+ cation is coordinated by four chloride anions which form hydrogen bonds with water molecules coordinated to $\text{Np}(\text{IV})$. According to DFT calculations, the three $\text{Np}^{4+}\text{--O}(\text{NpO}_2^+)$ bonds dissociate if the chloride ions or the water molecules are removed. The electronic population analysis shows that the electronic charge which stabilizes the $\text{Np}^{4+}\text{--NpO}_2^+$ interaction originates from the chlorine atoms. A part of the charge ends up in neptunyl species which become slightly negatively charged in the complex. This results in the diminution of electrostatic repulsion between $\text{Np}(\text{IV})$ and $\text{Np}(\text{V})$. The other flow of charge ends up in $\text{Np}(\text{IV})$ and involves a significant charge transfer through the neptunyl species toward the vacant 7s, 6d, and 5f $\text{Np}(\text{IV})$ orbitals. Additional stabilization in the system is brought by the water molecules which create hydrogen bonds with chloride ions.

In the crystal, the interaction between Np^{4+} and NpO_2^+ is strong enough to induce a significant lengthening of ~ 0.1 Å of the oxo bond in NpO_2^+ , involving the bond between Np^{4+} and (NpO_2^+) , compared to the second oxo bond. Frequency calculations and NBO analysis confirm the weakening of this oxo bond with a decrease of the neptunium 6d and 5f atomic orbital contribution to the σ and π oxo bonds upon binding to $\text{Np}(\text{IV})$.

Acknowledgment. The authors are grateful to CEA/DEN/DSOE/RB for the financial support.

Supporting Information Available: Additional information as noted in the text. This material is available free of charge via the Internet at <http://pubs.acs.org>.